Fermi surface of Pd and Pt under homogeneous strain

C. Cavalloni, W. Joss, and R. Monnier
Laboratorium für Festkörperphysik, Eidgenössische Technische Hochschule, CH-8093 Zürich, Switzerland

T. Jarlborg
Département de Physique de la Matière Condensée, Université de Genève, CH-1211 Genève, Switzerland
(Received 31 August 1984)

The response of the Fermi surface (FS) of the transition metals palladium and platinum to a homogeneous uniaxial deformation of the lattice has been investigated in detail experimentally and theoretically. The uniaxial-stress dependence of several extremal cross-sectional areas of the Fermi surface of $_{46}$Pd and $_{78}$Pt were obtained by a simultaneous measurement of the oscillatory magnetostriction and the de Haas—van Alphen torque. For six of the seven experimentally studied orbits in Pd, all the uniaxial-stress derivatives were determined and their sum compares well with the direct measurements of the hydrostatic-pressure derivatives by other authors. In Pt, four orbits on all three Fermi-surface sheets were investigated. Our result for the hydrostatic-pressure dependence of the Γ-centered electron orbit is again in agreement with a previously published direct estimate. From the experiments, the response of the FS to volume-conserving tetragonal shears and volume changes has been extracted and compared with self-consistently computed tetragonal shear (and, for Pt, volume) derivatives. The calculations, done with the linear combination of muffin-tin orbitals method, show that the discrepancy between theory and experiment for the shear response cannot be attributed to a failure of the rigid-muffin-tin approximation, as was stated in earlier work.

I. INTRODUCTION

The equilibrium Fermi surfaces (FS) of the $4d$ transition metal palladium and its $5d$ counterpart, platinum, are very similar, except for the small L-centered hole pocket which occurs only in the former element. Accurate de Haas—van Alphen measurements[1–3] have confirmed the topology predicted by first-principles band-structure calculations,[4–9] and the agreement between measured and self-consistently calculated extremal areas is fair.[8,9]

The first experimental investigation of the response of the FS of $_{46}$Pd and $_{78}$Pt to a homogeneous strain was that of Vuillemin and Bryant,[10] who studied the pressure dependence of the Γ-centered electron sheet by means of the fluid-helium phase-shift technique. More detailed measurements of the volume dependence of the FS of Pd were made by Skriver *et al.*,[8] using solid helium as a pressure medium. By combining the amplitude of the oscillatory magnetostriction and of the de Haas—van Alphen torque, Joss and van der Mark[11] were able to determine the uniaxial-stress derivatives of a number of orbits on the FS of palladium. Their findings can be compared with the uniaxial-strain dependences from a simultaneous measurement of the oscillations in the magnetization and in the sound velocity.[12,13]

The purpose of this paper is (i) to present the results of our comprehensive study of the uniaxial-stress dependence of the FS of Pd and Pt, (ii) to compare the resulting volume and tetragonal shear derivatives with the predictions of self-consistent band-structure calculations, and finally (iii) to repeat this comparison for the shear dependence of the FS of Pd, for which the theoretical volume dependence was studied in detail by Skriver *et al.*,[8] following an earlier non-self-consistent calculation by Das *et al.*[14]

II. EXPERIMENT

A. Measurement of the uniaxial-stress dependence

The uniaxial-stress dependence of a Fermi-surface cross section can be measured by combining the amplitude of the oscillatory magnetostriction and the de Haas—van Alpen (dHvA) torque.[15] Advantage is taken of the oscillatory behavior of the thermodynamic functions of an electron gas in a homogeneous magnetic field. To derive the oscillatory contribution to the potentials it proves convenient to use the thermodynamic potential Ω expressed in its independent variables: temperature T, volume V, chemical potential (Fermi energy) ζ, and magnetic field strength $\mathbf{H}$. Except for metals with a small number of carriers, the oscillations of $\zeta(H)$ needed to conserve the number of particles are weak compared to the value of the Fermi energy at zero field and ζ can be assumed to be field independent. The oscillatory contribution $\tilde{\Omega}$ to the thermodynamic potential Ω arising from one extremal cross-sectional area is then given by an expression originally derived by Lifshitz and Kosevich,[16]

$$\tilde{\Omega}=\sum_{r=1}^{\infty}\Omega_r\cos(\tfrac{1}{2}\pi r\mu g)\cos[2\pi r(F/H-\delta)\mp\tfrac{1}{4}\pi]\ , \qquad (1)$$

where g is the orbit-averaged electronic cyclotron g factor, and δ is the Onsager phase factor, equal to $\frac{1}{2}$ for free electrons. $\tilde{\Omega}$ varies periodically in H^{-1} with the dHvA frequency $F=\hbar cA/2\pi e$, where A is the extremal cross-sectional area of the Fermi surface normal to $\mathbf{H}$. The am-

plitude factor Ω_r depends on the ratio $\mu=m_c/m$ of the cyclotron effective mass to its free-electron value, on the Dingle temperature X_D, which is an orbital average of the scattering rate around the orbit, on the Fermi-surface curvature factor $|\partial^2 A/\partial k_H^2|$, and on H and T in the following way:

$$\Omega_r = DT\left[\frac{H}{r}\right]^{3/2}\left|\frac{\partial^2 A}{\partial k_H^2}\right|^{-1/2}\frac{\exp(-r\lambda\mu X_D/H)}{\sinh(r\lambda\mu T/H)}\,, \tag{2}$$

where the precise form of D may be found in the review of Shoenberg,[17] and $\lambda=14.69$ T/K is a constant.

For the derivation of the oscillatory magnetostriction we have to include in the thermodynamic potential the elastic energy density of the crystal lattice. In our experiments the temperature, the pressure, and the number N of particles are kept constant. The appropriate potential is therefore the Gibbs free energy G rather than the thermodynamic potential Ω. Compared to the full potential, its oscillatory part is small and the variation of this contribution with respect to a parameter (e.g., stress) will be identical for all thermodynamic functions provided the appropriate independent variables are kept constant.[18] The oscillatory strain $\tilde{\epsilon}_i$ measured parallel to the crystallographic axis i is then given by

$$\tilde{\epsilon}_i = -\left[\frac{\partial\tilde{G}}{\partial\sigma_i}\right]_{T,p,H,N} = -\left[\frac{\partial\tilde{\Omega}}{\partial\sigma_i}\right]_{T,V,H,\zeta}\,. \tag{3}$$

If we differentiate Eq. (1) with respect to the uniaxial stress σ_i, we find

$$\begin{aligned}\tilde{\epsilon}_i = &\sum_{r=1}^{\infty}\Omega_r 2\pi r\frac{F}{H}\frac{d\ln A}{d\sigma_i}\cos(\tfrac{1}{2}\pi r\mu g)\sin[2\pi r(F/H-\delta)\mp\tfrac{1}{4}\pi]\\ &+\sum_{r=1}^{\infty}\Omega_r\tfrac{1}{2}\pi r\mu g\frac{d\ln(\mu g)}{d\sigma_i}\sin(\tfrac{1}{2}\pi r\mu g)\cos[2\pi r(F/H-\delta)\mp\tfrac{1}{4}\pi]\\ &-\sum_{r=1}^{\infty}\frac{\partial\Omega_r}{\partial\sigma_i}\cos(\tfrac{1}{2}\pi r\mu g)\cos[2\pi r(F/H-\delta)\mp\tfrac{1}{4}]\,.\end{aligned} \tag{4}$$

The second term contains the stress dependence of the spin-splitting factor, and the last term the stress dependences of $|\partial^2 A/\partial k_H^2|$, the effective mass and the Dingle temperature. These terms contribute to the oscillatory strain with oscillations shifted by $\pi/2$ with respect to ones originated from the stress dependence of the extremal cross-sectional area A. Close to a spin-splitting zero $\frac{1}{2}\pi r\mu g=(n+\frac{1}{2})\pi$, the second term gains in importance relative to the first and last terms. Whether it is detectable or not will depend on the size of $d\ln(\mu g)/d\sigma$, which is not expected to vary substantially over a Fermi surface sheet. We want to stress, however, that if $d(\mu g)/d\sigma_i$ is a sizable fraction of $4(F/H)d\ln A/d\sigma_i$, this term must be considered everywhere on the Fermi surface sheet in question, and not only at spin-splitting zeros as mentioned by Finkelstein[19] and Griessen and Sorbello.[15] Equation (4) assumes that the Onsager phase factor is stress independent, as for free electrons, which is supported by the fact that in all metals studied so far, δ was found equal to $\frac{1}{2}$ within the experimental uncertainty.[17]

Very little is known about the stress dependences of the parameters in the second and in the last terms of Eq. (4). If we assume they are of the same order of magnitude as or smaller than the stress dependence $d\ln A/d\sigma_i$, the first term becomes dominant as long as the number F/H of occupied Landau tubes is large enough. Small areas are generally studied at low fields for which F/H is typically of the order of 10^2 to 5×10^3. Equation (4) then takes the simple form

$$\tilde{\epsilon}_i = -\frac{\partial\tilde{\Omega}}{\partial\ln A}\frac{d\ln A}{d\sigma_i}\,. \tag{5}$$

If the extremal area normal to **H** varies with the direction of H, the oscillatory magnetization

$$\tilde{\mathbf{M}} = -(\nabla_{\mathbf{H}}\tilde{\Omega})_{T,V,\zeta} \tag{6}$$

is not parallel to **H**, and there will be a torque per unit volume $\tilde{\tau}=\tilde{\mathbf{M}}\times\mathbf{H}$ acting on the sample. If we measure the component $\tilde{\tau}$ about an arbitrarily chosen suspension axis perpendicular to the field, and the angle ϕ is measured in a plane perpendicular to the suspension axis and specifies the orientation of the sample with respect to H, then $\tilde{\tau}$ is given by replacing σ with ϕ and $\tilde{\epsilon}$ with $-\tilde{\tau}$ in Eq. (4). For sufficiently large values of F/H, we get by analogy with Eq. (5),

$$\tilde{\tau} = \frac{\partial\tilde{\Omega}}{\partial\ln A}\frac{d\ln A}{d\phi}\,, \tag{7}$$

and combining the expression (5) and (7) we find for the stress dependence of the extremal cross-section area

$$\frac{d\ln A}{d\sigma_i} = -\frac{\tilde{\epsilon}_i}{\tilde{\tau}}\frac{d\ln A}{d\phi}\,. \tag{8}$$

The amplitudes of the oscillatory quantities are measured at the same temperature, orientation, and magnetic field strength, and the relative phase between $\tilde{\epsilon}_i$ and $\tilde{\tau}$ determines the sign of the stress dependence. $\tilde{\tau}$ and the $d\ln A/d\phi$ often vanish for a field applied along a symmetry axis but their quotient $\tilde{\tau}/(d\ln A/d\phi)$ can be accurately extrapolated from measurements of the two quantities as a function of the magnetic field orientation.

The main limitation of the method arises from torque-induced length changes. They can be minimized by using a sample which is short relative to its thickness. These spurious effects are easily detected by measuring the amplitude of the oscillatory magnetostriction as a function of

ϕ through symmetry planes or axes. If $A(\phi)$ has an extremum in the chosen symmetry direction, then the relative length change must be a symmetric function of ϕ about that direction. Any deviation from symmetry can be attributed to torque effects.

The oscillatory magnetostriction and the de Haas–van Alphen torque were simultaneously measured with a dilatorquemeter.[20] The measurements were done at 1.4 K in magnetic fields up to 10.5 T. The signals were digitized to allow Fourier analysis of the oscillations into frequency-dependent amplitude and phase. More experimental details may be found in Ref. 21.

B. Experimental procedure and results for Pd

The Fermi surface of Pd consists of four sheets.[1] Three of these contain holes (the X-centered fourth-band pockets, the L-centered fifth-band pockets, and the fifth-band open-hole sheet "scaffolding") and one contains electrons (the Γ-centered sixth-band sheet). Pd being a compensated metal, the volume of the electron sheet is equal to that of the three hole sheets with the X- and L-centered pockets providing only 1.8% of the hole contribution.[1] The scaffolding was not investigated in this work because of the very high effective masses[2] ($\mu = 2.3$ to 16) necessitating temperatures below 1 K or fields above 10 T.

The starting material of our sample had a quoted total impurity content of 6 ppm with less than 2 ppm of iron. A floating-zone technique was used to make the single

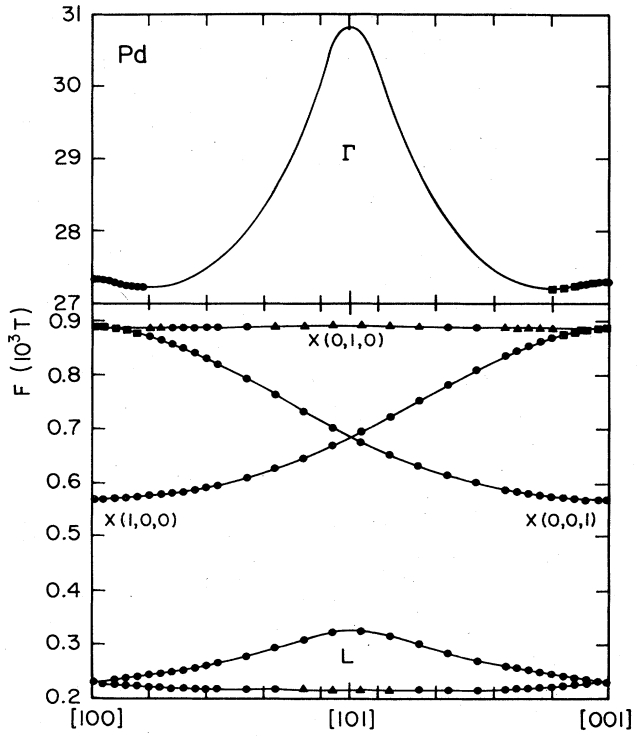

FIG. 1. de Haas–van Alphen frequencies in the (010) plane of palladium, determined from magnetostriction and torque. A circle denotes observation in both effects, a triangle only in magnetostriction, a square only in torque.

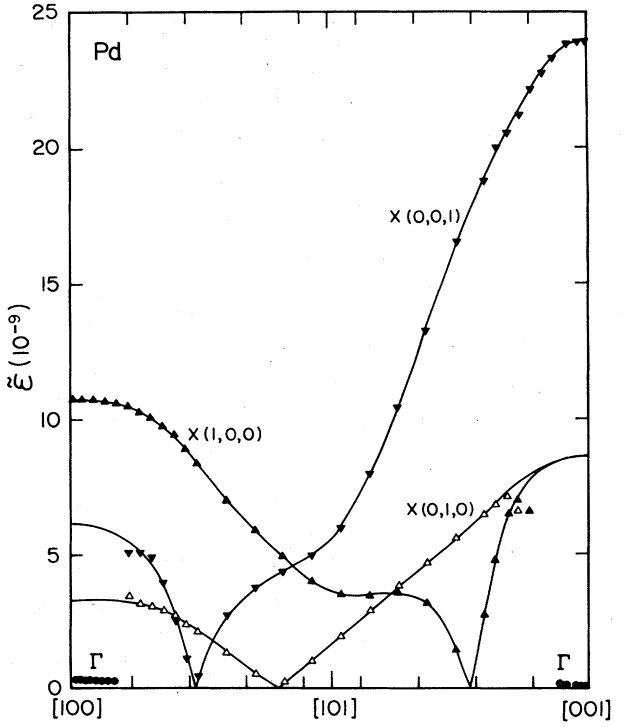

FIG. 2. Amplitude of magnetostrictive oscillations in the [001] direction in palladium at 1.4 K as a function of magnetic field orientation, for magnetic fields in the (010) plane. The values quoted are averages over optimum ranges of magnetic field intensity (see text).

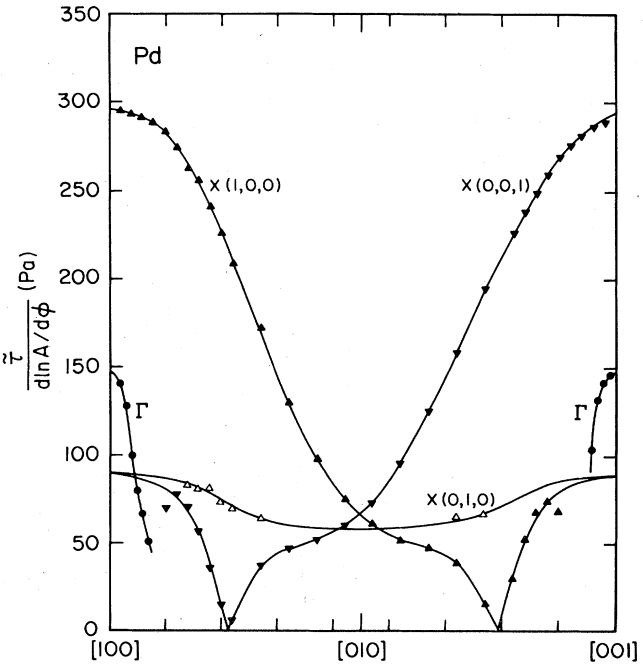

FIG. 3. de Haas–van Alphen torque in palladium normalized to relative change in area with field orientation as a function of the latter. Data obtained at 1.4 K and for different field ranges (see text).

crystal. The sample was subsequently annealed in air at 1100 °C, which increased the residual resistivity ratio by a factor of 2.5. The final ratio was 5000. To test the quality of our sample we have measured the Dingle temperature of two orbits on the X-centered hole pocket, and found it to be smaller than 0.15 ± 0.10 K.

The uniaxial stress dependence was measured on a single-crystal specimen of cylindrical shape 6 mm in diameter and 10 mm long. The magnetostrictive length change $\tilde{\epsilon}_i$ was recorded along the cylinder axis, which was parallel within 2° to the [001] crystallographic direction. The torque was measured about [010] as well as about the $[1\bar{1}0]$ direction, which is also the rotation axis of the dilatorquemeter in the magnetic field. The frequencies of the torque and magnetostriction oscillations are shown in Fig. 1 for magnetic fields in the (010) plane. In high-symmetry directions they are in excellent agreement with recently published high-precision measurements of Dye *et al.*[1] The amplitudes of the relative length changes as a function of magnetic field orientation in the (010) plane are shown in Fig. 2 for the orbits on the Γ-centered electron sheet and on the X-centered hole pockets. The corresponding quantity $\tilde{\tau}/(d\ln A/d\phi)$ occurring in the expression for the stress dependence, which is in our experimental configuration the product of magnetization and magnetic field, is displayed in Fig. 3. The values quoted for both effects are averages over a certain range of magnetic field strength (for X, 6.2—10.3 T; for Γ, 9.8—10.3 T) so as to optimize the signal. The oscillatory magnetostriction was so small compared to the large steady magnetostriction with quadratic field dependence, that we had to improve the dynamic range for the measurements of the oscillatory-length change. The change in dilatometer capacitance produced by the steady magnetostriction was compensated with help of a second torquemeter located in the magnetic field close to the sample and connected in parallel with the dilatometer. By driving a current proportional to the magnetic field through the coil attached on this torquemeter, a quadratic dependence of H of its capacitance is achieved, which cancels the undesired effect.

For a given orbit, the amplitudes in Figs. 2 and 3 show a qualitatively similar angular dependence. The torque amplitudes have cubic symmetry, and the length changes have tetragonal symmetry. For the X-centered hole pocket both amplitudes vanish for magnetic fields in the (010) plane, 21° from the [100] and [001] direction. This zero is associated with the spin splitting of the Landau levels, with an effective g factor of $1.03+2.06n$ using $\mu=0.97$ from Ernest and Joss.[22] For the same pocket, a further zero, only visible in the amplitude of the oscillatory magnetostriction, can be ascribed to a change in the sign of the stress dependence. The total derivative $d\ln A/d\sigma_{001}$ calculated with Eq. (8) from torque and length change is shown in Fig. 4. For the determination of the stress dependence of the L pocket, similar measurements were made with magnetic fields in the $(1\bar{1}0)$ plane. The uniaxial stress dependences in high-symmetry directions are summarized in Table I. The cross sections of the Γ, X, and L sheets can be recognized by their extremal frequencies (see Dye *et al.*[1]). The measurements on the Γ-centered electron sheet are made rather difficult by the high effective mass ($m_c^* \simeq 2$) and the small magnetostriction. The value for the orbit perpendicular to the stress direction is at the detection limit of our apparatus ($\Delta l/l \simeq 4.10^{-11}$). The Γ sheet allows for a central and a noncentral orbit in the [111] direction, and both have practically the same stress dependence. The large noncentral orbit gives a smaller signal and our resulting number is less reliable. Our measurements are most complete for the X-centered hole pocket. The results for the minimal orbit can be compared to those obtained by Caro *et al.*[13] from their measurement of the strain dependence.[23] Provided these results are correct, the discrepancy between the two sets of values can only be explained by an error of the order of 10% in the elastic constants of Table II.

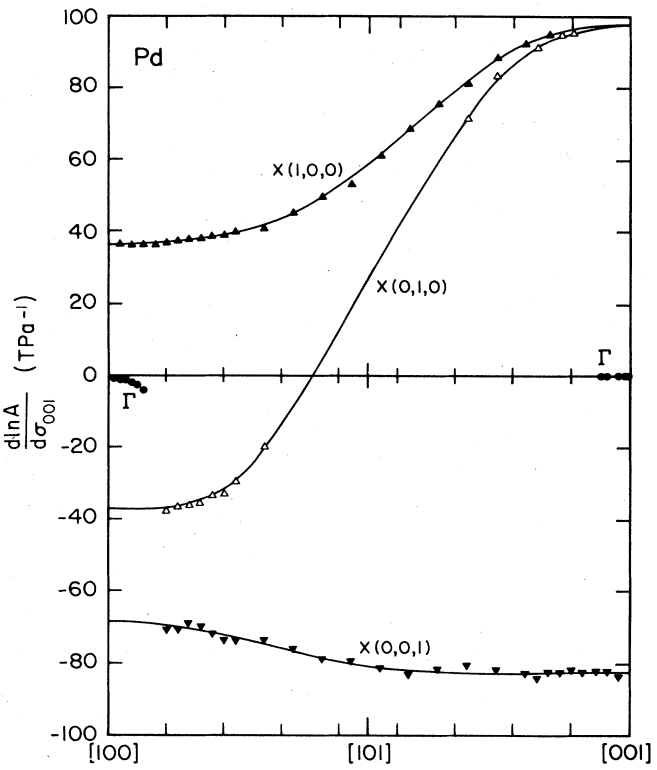

FIG. 4. Uniaxial-stress dependence along the [001] direction of extremal cross sections of the Fermi surface of palladium as a function of field orientation, for magnetic fields in the (010) plane.

From the uniaxial stress dependences we have calculated the pressure derivatives which we compare with the available direct measurements.[8,10] The agreement is quite satisfactory for the Γ and X sheets. The large uncertainty in the pressure dependences calculated from uniaxial stress data for the X pockets is due to the cancellation of large terms in the summation. The value for the L pocket of Skriver *et al.*[8] with magnetic field in [100] direction cannot be directly compared with our measurements, but at least gives an indication of the anomalous sign. The unusual negative-pressure derivative is discussed by

TABLE I. Experimental stress and hydrostatic-pressure derivatives of extremal cross-sectional areas of the Fermi surfaces of Pd and Pt.

	FS sheet:	Orbit-type	Center	Field	Area	Stress	$\frac{d\ln A}{dp}$ (TPa^{-1})		
Metal	orbit	band	$(2\pi/a)$	direction	(a.u.)	σ_{hkl}	$\frac{d\ln A}{d\sigma_{hkl}}$ (TPa^{-1})	$-\sum_i^3 \frac{d\ln A}{d\sigma_i}$	Direct measurements
Pd	X pocket	h_4	$X(1,0,0)$	[100]	0.0153	σ_{100}	-82.5 ± 2[a]	10.5 ± 2[a]	10.5 ± 0.7[b]
							-102 ± 6[c]	7.2 ± 1[c]	
						$\sigma_{010},\sigma_{001}$	36 ± 1[a]		
							48 ± 3[c]		
				[010]	0.0238	σ_{100}	-68 ± 3[a]	7 ± 8[a]	6.1 ± 0.7[b]
						σ_{010}	98 ± 4[a]		
						σ_{001}	-37 ± 6[a]		
Pd	L pocket	h_5	$L(\frac{1}{2},\frac{1}{2},\frac{1}{2})$	[100]	0.006 14	σ_{100}	44 ± 6[c]	-21.4 ± 1[c]	-17 ± 2[b]
						$\sigma_{010},\sigma_{001}$	-11 ± 3[c]		
				[111]	0.005 08	$\sigma_{100},\sigma_{010},\sigma_{001}$	11.5 ± 6[a]	-34.5 ± 10[a]	
				[11$\bar{2}$]	0.008 69	σ_{001}	300 ± 80[a]		
Pd	Electron sheet	e_6	$\Gamma(0,0,0)$	[100]	0.7311	σ_{100}	0.1 ± 0.3[a]	3.7 ± 0.5[a]	4.0 ± 0.4[d]
						$\sigma_{010},\sigma_{001}$	-1.9 ± 0.3[a]		4.1 ± 0.8[b]
				[111]	0.6480	$\sigma_{100},\sigma_{010},\sigma_{001}$	-1.2 ± 0.3[a]	3.6 ± 0.5[a]	3.9 ± 0.4[d]
			Λ[e]	[111]	0.6859	$\sigma_{100},\sigma_{010},\sigma_{001}$	-1.3 ± 0.6[a]	3.9 ± 1[a]	
Pt	X pocket	h_4	$X(1,0,0)$	[100]	0.002 98	σ_{100}	-188 ± 6[fg]	39 ± 8[f]	
						$\sigma_{010},\sigma_{001}$	74.5 ± 4[fg]		
				[010]	0.004 63	σ_{100}	-174 ± 7[f]	68 ± 9[f]	
						σ_{010}	67.8 ± 3[f]		
						σ_{001}	37.8 ± 5[f]		
Pt	Open holes: α	h_5	$W(\frac{1}{2},0,1)$	[100]	0.0740	σ_{100}	81.7 ± 2[f]	5.3 ± 2[f]	
						$\sigma_{010},\sigma_{001}$	-43.5 ± 1[f]		
Pt	Electron sheet	e_6	$\Gamma(0,0,0)$	[100]	0.770	σ_{100}	3.3 ± 1[f]	2.7 ± 2[f]	3.2 ± 0.3[d]
						$\sigma_{010},\sigma_{001}$	-3.0 ± 1[f]		
				[111]	0.687				2.8 ± 0.3[d]

[a]This work and Ref. 11.
[b]Skriver *et al.* (Ref. 8).
[c]Obtained from strain dependences by Caro *et al.* (Refs. 13 and 23) using the elastic constants of Table II.
[d]Vuillemin and Bryant (Ref. 10).
[e]Noncentral orbit.
[f]This work.
[g]Determined from the second dHvA harmonic.

Skriver *et al.*,[8] who attribute this behavior to the volume dependence of the *sp-d* hybridization.

C. Experimental procedure and results for Pt

The Fermi surface of Pt is similar to the one of Pd, except that the L-centered hole pockets are missing. The fifth-band "scaffolding" and the sixth-band, Γ-centered electron sheet have an 11% larger volume than in Pd, and the X-centered hole pockets only contain 0.11% of the holes.[3] The cyclotron effective masses on the scaffolding are about 70% smaller than in Pd, and representative orbits on all three Fermi surface sheets have been investigated.

The Pt single crystal was obtained from Materials Research Corporation. The sample was annealed for 60 h in an oxygen atmosphere at 1500 °C, which increased its residual resistivity ratio from 270 to 700. We measured two Dingle temperatures and obtained $X_D=0.5\pm 0.05$ K for an orbit on the X pocket, and $X_D=0.8\pm 0.05$ K for the α orbit on the scaffolding.

The crystal was oriented within 1° along the [001] direction, and cut by spark erosion to a cylindrical specimen with 4.6 mm in diameter and 5.3 mm in length. After spark erosion the specimen was etched in aqua-regia. The oscillatory magnetostriction was measured along the cylinder axis and the torque was measured about the [010] direction, which is the axis about which the dilatorquemeter can be rotated in the field. The frequencies of the magnetostrictive and torque oscillations as a function of field orientation are shown in Fig. 5. The frequency branches (α,γ,δ) from orbits on the scaffolding are labeled in the standard way.[3] In high-symmetry directions they are in excellent agreement with the measurements of Dye *et al.*[3] The α orbit on the scaffolding ceases to exist for field angles larger than 39° from [100] or [001] in the (010) plane, 2.5° further away than reported by Ketterson and Windmiller.[24]

The amplitude of the relative length changes as a func-

TABLE II. Equilibrium parameters for Pd and Pt at 0 K.

		Pd	Pt
Lattice constant	a (Å)	3.8782[a]	3.9164[b]
	a (a.u.)	7.3287[a]	7.4009[b]
Elastic stiffness constants	C_{11} (GPa)	233.3[c]	358.0[d]
	C_{12} (GPa)	175.3[c]	253.6[d]
	C_{44} (GPa)	71.3[c]	77.4[d]
Elastic compliance constants	S_{11} (TPa^{-1})	12.07[c]	6.77[d]
	S_{12} (TPa^{-1})	−5.18[c]	−2.81[d]
Compressibility	κ (TPa^{-1})	5.14[c]	3.47[d]

[a]H. W. King and F. D. Manchester, J. Phys. F **8**, 15 (1978).
[b]The room-temperature lattice constant [W. B. Pearson, *Handbook of Lattice Spacings and Structures of Metals and Alloys* (Pergamon, Oxford, 1967), Vol. 2, p. 86] is converted to 0 K with thermal expansion data [Y. S. Touloukian, R. K. Kirby, R. E. Taylor, and P. D. Desai, in *Thermal Expansion-Metallic Elements and Alloys, Thermophysical Properties of Matter,* edited by Y. S. Touloukian (IFI/Plenum, New York, 1975), Vol. 12, p. 254].
[c]Average of J. A. Rayne, Phys. Rev. **118**, 1545 (1960); E. Walker, J. Ortelli, and M. Peter, Phys. Lett. **31A**, 240 (1970); and D. K. Hsu and R. G. Leisure, Phys. Rev. B **20**, 1339 (1979).
[d]R. E. MacFarlane, J. A. Rayne, and C. K. Jones, Phys. Lett. **18**, 91 (1965).

tion of magnetic field orientation in the (010) plane is shown in Fig. 6, and the amplitude factor $\tilde{\tau}/(d\ln A/d\phi)$ is shown in Fig. 7. The angular dependence $d\ln A/d\phi$ was determined from the measured de Haas–van Alphen frequency with a typical accuracy of 2%. The values quoted in Figs. 6 and 7 correspond to averages over certain range of magnetic field strength (X, 6.2–10.3 T; α,Γ, 10.0–10.3 T). The signals from the X pockets reveal a remarkably strong harmonic content. For the minimal orbit the amplitude of the second dHvA harmonic is even stronger than the fundamental one. The second harmonic originating from the $X(1,0,0)$ pocket [similarly for the $X(0,0,1)$ pocket] shows spin-splitting zeros at 53° and 78° from [100] in the (010) plane. At about 65°, the angular dependence of both amplitudes goes through a local maximum, which means the magnitude of the spin-splitting factor $\cos(\pi r\mu g/2)$ for $r=1$ and 2 is 1. The decrease of the fundamental amplitude near the [100] and [001] direction can therefore be explained by the argument of the cosine going toward $(n+\frac{1}{2})\pi$. The strong angular dependence of the spin-splitting enhances the effect of a slight misalignment of the plane of rotation of the field, resulting in a small deviation from cubic symmetry for the torque amplitudes.

For the α-orbit a spin-splitting zero is found for magnetic fields in the (010) plane, 21° from the [100] and [001] direction. Ketterson and Windmiller[24] and Nordborg *et al.*[25] found this zero at 23° from [100] or [001] in a purer sample. Nordborg *et al.* proved that 80 ppm of iron are enough to shift the zero back to 21°.

The stress dependence $d\ln A/d\sigma_{001}$ calculated with Eq. (8) is shown in Fig. 8. For the minimal orbit on the $X(1,0,0)$ and $X(0,0,1)$ pockets the $d\ln A/d\sigma_{001}$ deter-

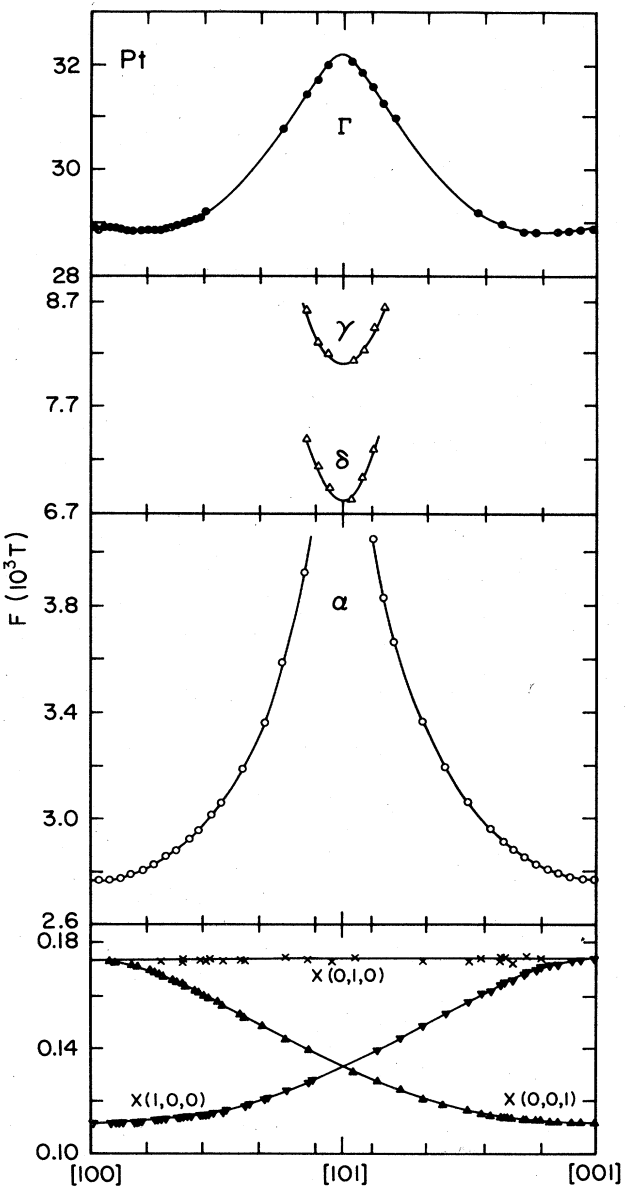

FIG. 5. de Haas–van Alphen frequencies in the (010) plane of platinum, determined from magnetostriction and torque.

mined from the fundamental and second harmonic of the signal give different values. For these orbits the number of Landau tubes $F/H=11-18$ is small, the spin-splitting factor of the fundamental frequency goes toward zero, and the second term in Eq. (4) containing the stress dependence μg becomes important. On the other hand, for the second harmonic the magnitude of the spin-splitting factor is 1 and the second term in Eq. (4) is small. We therefore quote in Table I for the stress dependences in high-symmetry directions the values obtained from the amplitudes of the second harmonic. To determine the stress dependence of the X (0,1,0) pocket we assumed that $\tilde{\tau}/(d\ln A/d\phi)$ was independent of ϕ (as suggested by Fig. 5) and equal to its value for the other X pockets at [100]

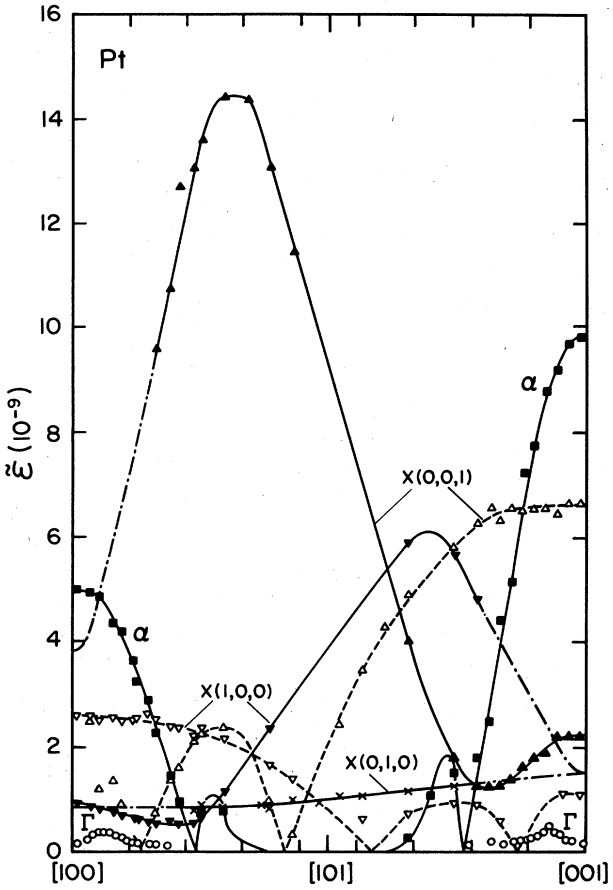

FIG. 6. Amplitude of magnetostrictive oscillations in the [001] direction in platinum at 1.4 K as a function of magnetic field orientation, for magnetic fields in the (010) plane. The values quoted are averages over optimum ranges of magnetic field intensity (see text). Data obtained from the second dHvA harmonic are represented by a dashed line, extrapolated values by a dotted-dashed line.

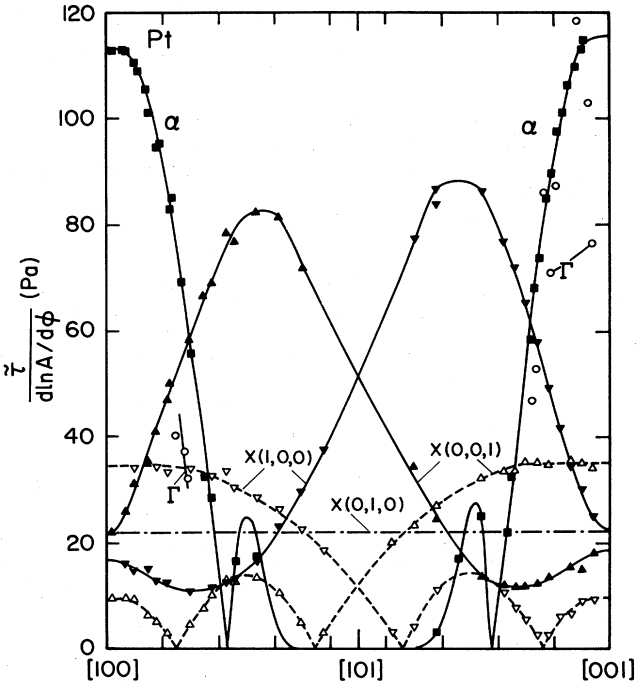

FIG. 7. de Haas–van Alphen torque in platinum normalized to relative change in area with field orientation as a function of the latter. Data obtained at 1.4 K and for different field ranges (see text). Data from the second dHvA harmonic are represented by a dashed line, extrapolated values by a dotted-dashed line.

and [001]. In contrast to Pd, no change of sign in $d\ln A/d\sigma_{001}$ was found for this pocket. The only available direct measurements of the pressure dependence are for the Γ-centered electron sheet,[10] and compare well with the admittedly inaccurate value obtained by summing our stress derivatives. No stress dependences could be obtained for the γ and δ orbits on the scaffolding.

III. METHOD OF CALCULATION

The measured uniaxial stress dependences were converted to volume and tetragonal shear derivatives, which are directly accessible to calculations. We have computed the band structure of palladium and platinum in the fcc structure and for a ±2% volume-conserving tetragonal shear along the [001] direction, using the linear combination of muffin-tin orbitals (LMTO) method.[26] Self-consistent semirelativistic calculations with a code developed by one of us (T.J.) produced potential parameters for the distorted structures which differed only insignificantly from the ones at equilibrium, as expected from the theorem of Gray and Gray,[27] according to which there are no first-order corrections in the strain for a potential of the muffin-tin or equivalently of the atomic sphere form. In the calculations presented here, the code developed by Skriver[28] and the potential parameters obtained self-consistently by Glötzel *et al.*[29] in the atomic sphere approximation to the LMTO method were used for all three structures.[30] Spin-orbit coupling and the so-called combined correction terms, which account for the proper shape of the Wigner-Seitz cell and higher partial waves, were also included. We have not taken into account the relativistic corrections to the exchange energy recently discussed in relation to the electronic structure of Pd and Pt in Ref. 9. They do not affect the FS of Pd, while improving the agreement with experiment for the heavier element Pt. They are most important close to the nucleus, and we do not expect them to influence the strain dependence significantly.

The natural unit cell for our problem is body-centered tetragonal spanned by the basis vectors $(a/2, a/2, 0)$, $(-a/2, a/2, 0)$, $(0,0,c)$, where $c=a$ in the undistorted case. However, with this convention, the extremal orbits on the FS are not immediately comparable with experiments, and the matrices to be diagonalized double in size. We therefore used the standard fcc unit cell and Brillouin zone (BZ) for the strained crystal also, allowing for the necessary volume-conserving distortions. For the determination of the Fermi energy E_F, the bands were comput-

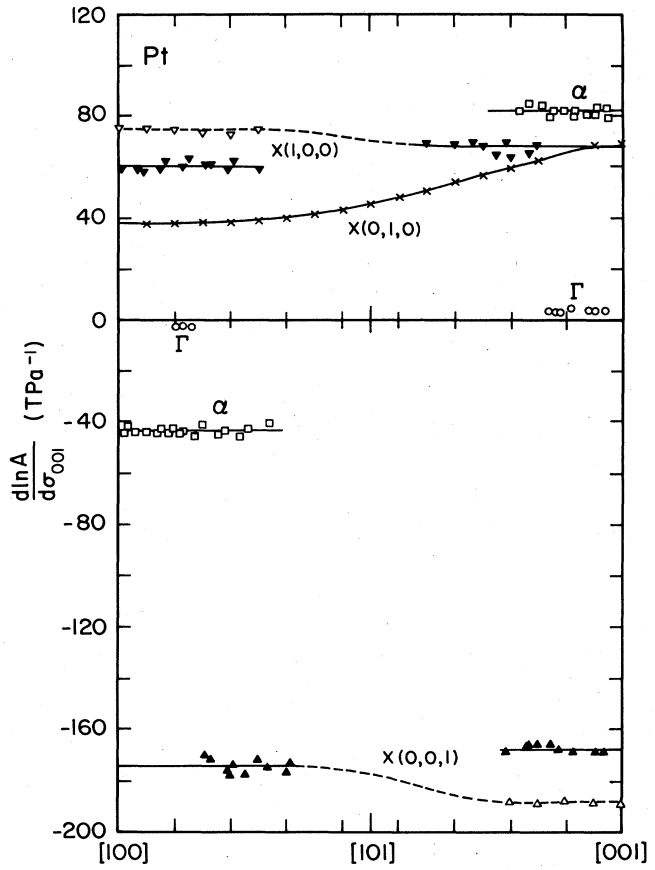

FIG. 8. Uniaxial-stress dependence along the [001] direction of extremal cross sections of the Fermi surface of platinum as a function of field orientation, for magnetic fields in the (010) plane. Data obtained from the second dHvA harmonic are represented by a dashed line.

ed at 625 points on a regular mesh in $\frac{1}{16}$ of the BZ (which is the volume of the irreducible part of the BZ for a [001] shear). In the distorted case, the mesh points in the immediate vicinity of the (111) symmetry plane through L had to be shifted slightly, in order to lie on the plane, given by the equation

$$k_x+k_y+\frac{k_z}{(1+\gamma_z)^{3/2}}=(1+\gamma_z)^{1/2}\left[1+\frac{1}{2(1+\gamma_z)^3}\right]. \tag{9}$$

The density-of-states functions were constructed with the tetrahedron integration method.[31] The above-mentioned shift in the k mesh led to tetrahedra of different sizes at the edge of the irreducible BZ, and the procedure was checked by computing the total volume of the irreducible part of the BZ as the sum over all tetrahedra.

For tracing a given orbit, a new mesh of k points was generated in the appropriate plane. The energy eigenvalues were computed for each point and the shape and area of the orbit were obtained from a two-dimensional linear interpolation between these first-principles values. The mesh size was chosen in such a way that each orbit typically involved 100 interpolated points. With this procedure, the error in the radius is quadratic in the mesh size, and our choice leads to a precision of the order of 0.5% for the extremal areas. The volume derivatives for Pt were obtained from band structures corresponding to changes in lattice spacing of 0% and ±1% of the theoretical value.

IV. RESULTS AND DISCUSSION

Our calculated extremal areas for Pd and Pt at equilibrium are compared with the measured ones in Table III. In the columns labeled "Shift," we also give the amount by which the theoretical Fermi energy has to be shifted in order to make the two areas coincide. For the large-area orbits, the agreement between theory and experiment is better than in Refs. 8 and 9. The computed areas of the hole orbits are all too big, especially for the X-centered pockets, where the discrepancy with experiment is of the order of 20% in Pd and 100% in Pt. The latter result is not surprising in view of the very small size of these pockets, and a similar difference was reported by Skriver *et al.*[8] for the L-centered hole pocket in Pd which is comparable in volume.

The Fermi energy did not change when the crystal was distorted, and we computed the shear derivatives both at E_F and at its shifted value to get an estimate of the effect of errors in extremal area on their strain response. Our theoretical results are summarized in Table IV together

TABLE III. Experimental and calculated areas of some extremal orbits on the Fermi surfaces of Pd and Pt. In the column labeled "Shift" we give the amount by which the calculated Fermi energy has to be shifted in order for the two values to coincide.

FS sheet: orbit	Orbit center	Field direction	Pd Area (a.u.) Expt.[a]	Pd Area (a.u.) Calc.	Pd Shift (mRy)	Pt Area (a.u.) Expt.	Pt Area (a.u.) Calc.	Pt Shift (mRy)
X pocket	$X(1,0,0)$	[100]	0.015 29	0.0184	2.7	0.002 98[b]	0.0060	4.4
		[010]	0.023 76	0.0304	3.2	0.004 63[c]	0.0091	4.4
Open holes: α	$W(\frac{1}{2},0,1)$	[100]	0.071 90	0.0825	1.3	0.0740[b]	0.0833	3.0
Electron sheet	$\Gamma(0,0,0)$	[100]	0.7312	0.732	−0.0	0.770[b]	0.772	−0.0

[a]Reference 1.
[b]Reference 3.
[c]This work.

TABLE IV. Experimental and theoretical tetragonal shear dependence of the area of some extremal orbits on the Fermi surfaces of Pd and Pt.

FS sheet: Orbit	Center ($2\pi/a$)	Field direction	i	$d\ln A/d\gamma_i$ Pd Expt.	Pd Calc.[a]	Pd Calc.[b]	Pd Calc.[c]	Pt Expt.[d]	Pt Calc.[a]	Pt Calc.[b]
X pocket	$X(1,0,0)$	[100]	x	-6.87 ± 0.17[d] -8.7 ± 0.5[e]	-8.4 ± 0.2	-9.8 ± 0.2	-10.3	-27.4 ± 1	-21.5 ± 0.3	-32.9 ± 0.3
			y,z	3.44 ± 0.09[d] 4.35 ± 0.25[e]	3.9 ± 0.2	4.5 ± 0.2	5.1	13.7 ± 0.5	10.0 ± 0.3	15.0 ± 0.3
		[010]	x	-5.7 ± 0.5[d]	-7.0 ± 0.2	-8.1 ± 0.3	-8.9	-23.7 ± 1	-18.5 ± 0.3	-28.7 ± 0.4
			y	8.7 ± 0.5[d]	10.8 ± 0.2	12.4 ± 0.3	12.1	14.2 ± 1	10.7 ± 0.3	15.7 ± 0.4
			z	-3.0 ± 0.5[d]	-4.4 ± 0.2	-5.0 ± 0.3	-3.2	9.5 ± 1	6.7 ± 0.3	10.9 ± 0.4
Open holes: α	$W(\frac{1}{2},0,1)$	[100]	x		15.5 ± 0.2	17.7 ± 0.2		13.1 ± 0.3	12.6 ± 0.2	15.7 ± 0.2
			y,z		-8.9 ± 0.2	-9.4 ± 0.2		-6.5 ± 0.2	-7.3 ± 0.2	-7.9 ± 0.2
Electron sheet	$\Gamma(0,0,0)$	[100]	x	0.12 ± 0.03[d]	0.1 ± 0.2	0.1 ± 0.2	0.21	0.66 ± 0.2	0.4 ± 0.2	0.4 ± 0.2
			y,x	-0.06 ± 0.02[d]	-0.0 ± 0.2	-0.0 ± 0.2	-0.10	-0.33 ± 0.1	-0.2 ± 0.2	-0.2 ± 0.2

[a]Calculated at the theoretical Fermi energy

[b]Calculated at the energy at which the equilibrium theoretical and experimental areas coincide (see Table III).

[c]KKR phase-shift parametrization of Ruesink *et al.* (Ref. 12).

[d]Obtained from the uniaxial stress dependences given in Table I using the relation $d\ln A/d\gamma_i=(C_{11}-C_{12})[d\ln A/d\sigma_i-\frac{1}{2}(d\ln A/d\sigma_j+d\ln A/d\sigma_k)]$, $(i,j,k=1,2,3;\ i\neq j\neq k)$, and the elastic stiffness constants of Table II.

[e]Obtained from the strain dependences by Caro *et al.* (Ref. 13) using the relation $d\ln A/d\gamma_i=d\ln A/d\epsilon_i-\frac{1}{2}(d\ln A/d\epsilon_j+d\ln A/d\epsilon_k)$, $(i,j,k=1,2,3;\ i\neq j\neq k)$.

with those obtained by Ruesink *et al.*[12] for Pd using the rigid-muffin-tin approximation (RMTA) and a Korringa-Kohn-Rostoker (KKR)—phase-shift parametrization scheme, and the experimental values. In both metals, theory and experiment agree on the very weak shear dependence of the Γ-centered orbit which reflects the fact that the sixth-band electron sheet is a distorted free-electron sphere. For Pd the calculations systematically overestimate the strain dependences of the X-centered hole pockets. Shifting the Fermi energy enhances all logarithmic derivatives by roughly the same factor $\simeq1.15$, the minimal (maximal) area being reduced by a factor $\simeq1.20$ (1.27) in that process. This means that for the minimal orbit most of the change in $d\ln A/d\gamma_i$ with energy is due to the change in extremal area, the energy dependence of $dA/d\gamma_i$ being much weaker. In Pt, where the effect of the energy shift is more dramatic due to the small size of the X pockets, the two factors are equally important: The extremal areas are divided by 2 and the logarithmic derivatives are multiplied by $\simeq1.5$ after the shift. Our calculated shear derivatives at the two values of E_F very nicely encompass the experimental ones. Note that they also reproduce the experimentally observed sign change in $d\ln A/d\gamma_z$ for the $x(1,0,0)$-centered orbit in the x-z plane when going from Pd to Pt. We have no simple explanation for this phenomenon, except that it must be related to the much larger sp-d hybridization and spin-orbit coupling in Pt. For the W-centered α orbit the agreement between theory and experiment is again very satisfactory. A check on the numerical consistency of our calculations is given by the exact sum rule, satisfied by construction in the approach of Ref. 12, according to which the sum of the three independent shear derivatives for a given orbit should vanish identically. In all cases a change of less than 10% in the derivatives would suffice to satisfy the sum rule.

Our computed volume dependences of extremal areas on the FS of Pt are listed in Table V, together with the experimental values obtained from the pressure derivatives of Table I. The biggest discrepancy between theory and experiment occurs for the W-centered α orbit, for which no accurate measurement exists. The large volume dependence of the X-centered hole pocket is an indication of the strong sp-d hybridization, as shown formally by Skriver *et al.*,[8] who derived the following formula:

$$\frac{d\ln A}{d\ln\Omega}=-\frac{2}{3}+\frac{(E_F-C)\pi\mu}{3A}\left[\frac{d\ln(E_F-C)}{d\ln S}+\alpha\right], \quad (10)$$

TABLE V. Experimental and theoretical volume derivatives of the area of some extremal orbits on the Fermi surface of Pt.

FS sheet: Orbit	Center ($2\pi/a$)	Field direction	$d\ln A/d\ln\Omega$ Expt.[a]	Calc.
X pocket	$X(1,0,0)$	[100]	-11.2 ± 2[b]	-11.9
		[010]	-19.6 ± 3[b]	-13.1
Open holes: α	$W(\frac{1}{2},0,1)$	[100]	-1.5 ± 0.6[b]	-0.81
Open holes: ϵ	$\Gamma(0,0,0)$	[100]		-0.75
Electron sheet	$\Gamma(0,0,0)$	[100]	-0.92 ± 0.1[c]	-0.96
		[110]		-1.03
		[111]	-0.81 ± 0.1[c]	-0.86

[a]Obtained from the hydrostatic pressure derivatives given in Table I using the relation $d\ln A/d\ln\Omega=(-1/\kappa)d\ln A/dp$ with the compressibility given in Table II.

[b]This work.

[c]Vuillemin and Bryant (Ref. 10).

where S is the Wigner-Seitz radius, μ is the cyclotron mass of the orbit, C is the center of gravity of the band under consideration, characterized by an intrinsic band mass m (denoted μ in Refs. 8 and 28), and $\alpha = d\ln(mS^2)/d\ln S$. For a pure d band the parenthesis on the right-hand side of Eq. (10) vanishes, and $d\ln A/d\ln\Omega = -\frac{2}{3}$. From the volume dependence of the potential parameters we find $\alpha = 5.18$, and according to our calculations $d\ln(E_F - C)/d\ln S = -4.79$, which, when inserted into (10) with our calculated effective masses yields $d\ln A/d\ln\Omega = -7.5$ for both extremal orbits on the X pocket, in qualitative agreement with the direct estimates given in Table V.

As a by-product of our calculation, we also obtain a value for the electronic Grüneisen parameter

$$\gamma_e = \frac{d\ln N(E_F)}{d\ln\Omega} , \tag{11}$$

where $N(E_F)$ is the density of states at the Fermi level, equal to 25.3 electrons/Ry atom at equilibrium, which compares well with the 24.8 electrons/Ry atom quoted by MacDonald *et al.*[9] Our result for γ_e is 1.0, somewhat lower than the value of 1.23 found by Skriver *et al.*[8] for Pd, and deviates strongly from the value $\alpha/3 = 1.73$ expected for a pure d band, pointing again at the importance of *sp-d* hybridization in Pt.

In summary, our experimental and theoretical study of the FS of Pt under homogeneous strain has demonstrated that the current band-structure ground-state formalism is capable of reproducing the measured changes in extremal areas, and that volume-conserving shears are well reproduced within the RMTA. A similar conclusion is implied by the comparison of our computed shear derivatives with experiment for Pd, so that the negative results reported in Ref. 12 must have another origin than the failure of the RMTA.

ACKNOWLEDGMENTS

We are grateful to Professor J. L. Olsen for his continued interest and support. The palladium crystal was generously supplied by Professor R. Griessen and Dr. E. Walker. One of us (R.M.) would like to express his long-due thanks to Dr. H. L. Skriver for having introduced him to the LMTO method and generously providing him with a copy of his computer code. Helpful correspondence with Dr. D. Glötzel at the early stages of this work is also gratefully acknowledged. This work benefited from the financial support of the Schweizerischer Nationalfonds zur Förderung der wissenschaftlichen Forschung.

[1]D. H. Dye, S. A. Campbell, G. W. Crabtree, J. B. Ketterson, N. B. Sandesara, and J. J. Vuillemin, Phys. Rev. B **23**, 462 (1981).

[2]W. Joss, L. N. Hall, G. W. Crabtree, and J. J. Vuillemin, Phys. Rev. B **30**, 5637 (1984).

[3]D. H. Dye, J. B. Ketterson, and G. W. Crabtree, J. Low Temp. Phys. **30**, 813 (1978), and references therein.

[4]O. K. Andersen and A. R. Mackintosh, Solid State Commun. **6**, 285 (1968).

[5]O. K. Andersen, Phys. Rev. B **2**, 883 (1970).

[6]F. M. Mueller, A. J. Freeman, J. O. Dimmock, and A. M. Furdyna, Phys. Rev. B **1**, 4617 (1970).

[7]T. J. Watson-Yang, A. J. Freeman, and D. D. Koelling, J. Magn. Magn. Mater. **5**, 277 (1977).

[8]H. Skriver, W. Venema, E. Walker, and R. Griessen, J. Phys. F **8**, 2313 (1978).

[9]A. H. MacDonald, J. M. Daams, S. H. Vosko, and D. D. Koelling, Phys. Rev. B **23**, 6377 (1981).

[10]J. J. Vuillemin and H. J. Bryant, Phys. Rev. Lett. **23**, 914 (1969).

[11]W. Joss and W. van der Mark, in *Proceedings of the International Conference on the Physics of Transition Metals, Toronto, 1977,* edited by M. J. G. Lee, J. M. Perz, and E. Fawcett (IOP, London, 1978), p. 74.

[12]W. Ruesink, J. de Wilde, R. Griessen, and M. J. G. Lee, J. Phys. (Paris) Colloq. **39**, C6-1097 (1978); and M. J. G. Lee (private communication).

[13]J. Caro, D. W. Ruesink, J. de Wilde, and M. J. G. Lee, as cited in W. Joss, R. Griessen, and E. Fawcett, *Electron States and Fermi Surfaces of Homogeneously Strained Metallic Elements,* Vol. 13b of *Landolt-Börnstein, New Series, Group III* (Springer, Berlin, 1983), p. 176.

[14]S. G. Das, D. D. Koelling, and F. M. Mueller, Solid State Commun. **12**, 89 (1973).

[15]R. Griessen and R. S. Sorbello, J. Low Temp. Phys. **16**, 237 (1974).

[16]I. M. Lifshitz and A. M. Kosevich, J. Exptl. Theoret. Phys. (U.S.S.R.) **29**, 730 (1955) [Sov. Phys.—JETP **2**, 636 (1956)].

[17]D. Shoenberg, *Magnetic Oscillations in Metals* (Cambridge University Press, Cambridge, 1984).

[18]L. D. Landau and E. M. Lifshitz, *Statistical Physics* (Pergamon, London, 1958), pp. 47,70.

[19]M. M. Finkelstein, J. Low Temp. Phys. **14**, 287 (1974).

[20]R. Griessen, M. J. G. Lee, and D. J. Stanley, Phys. Rev. B **16**, 4385 (1977).

[21]W. Joss, Phys. Rev. B **23**, 4913 (1981).

[22]D. Ernest and W. Joss, in *Physics of Transition Metals, 1980,* edited by P. Rhodes (IOP, London, 1981), p. 463.

[23]The slight difference between the stress derivatives of Caro *et al.* quoted in Table I and those given in Ref. 13 stems from our use of better elastic constants.

[24]J. B. Ketterson and L. R. Windmiller, Phys. Rev. B **2**, 4813 (1970).

[25]L. Nordborg, M. Dronjak, K. Gramm, and S. P. Hörnfeldt, J. Magn. Magn. Mater. **23**, 323 (1981).

[26]O. K. Andersen, Phys. Rev. B **12**, 3060 (1975).

[27]D. M. Gray and A. M. Gray, Phys. Rev. B **14**, 669 (1976).

[28]H. L. Skriver, *The LMTO Method* (Springer, Berlin, 1984).

[29]D. Glötzel, O. K. Andersen, and O. Jepsen, Adv. Phys. (to be published).

[30]The lattice parameters used in Ref. 29 (Pd, 7.3517 a.u.; Pt; 7.4131 a.u.) differ slightly from the experimental ones at 0 K given in Table II. This does not affect the relative change of extremal areas under a volume conserving shear. The areas at the correct lattice spacing were obtained from the volume dependences computed for Pd in Ref. 8 and for Pt in this work.

[31]O. Jepsen and O. K. Andersen, Solid State Commun. **9**, 1763 (1971).